

## *Geodetic constraints on contemporary deformation in the northern Walker Lane: 2. Velocity and strain rate tensor analysis*

Corné Kreemer\*  
Geoffrey Blewitt  
William C. Hammond

*Nevada Bureau of Mines and Geology, and Seismological Laboratory, University of Nevada, Reno, Nevada 89557-0178, USA*

### ABSTRACT

We present a velocity and strain rate model for the northern Walker Lane derived from a compilation of geodetic velocities and corrected for transient effects owing to historic earthquakes on the Central Nevada seismic belt. We find that from 37°N to 40°N, the Walker Lane is characterized by an ~100-km-wide zone with near-constant strain rates associated with ~10 mm yr<sup>-1</sup> total motion across the zone. The strain rates depict predominantly shear deformation, but south of 39°N, the extensional component of the strain rate tensor increases and thus reflects more of a transtensional domain there. We conclude that this transtension is a kinematic consequence of the motion of the Sierra Nevada–Great Valley block, which is not parallel to its eastern margin, i.e., the eastern Sierra front, south of 39°N. While the orientations of several normal and strike-slip faults in the Walker Lane region are consistent with the strain rate model results at several places, the mode and rate at which geologic structures accommodate the deformation are less clear. Left-lateral faulting and clockwise rotations there may contribute to the accommodation of the velocity gradient tensor field, and most normal faults are properly oriented to accommodate some component of the regional shear strain, but significant additional right-lateral strike-slip faulting is required to accommodate the majority of the 10 mm yr<sup>-1</sup> relative motion. Overall, the along-strike variation in the active tectonics of Walker Lane suggests that (1) various mechanisms are at play to accommodate the shear, (2) parts of the surface tectonics may (still) be in an early stage of development, and (3) inherited structural grain can have a dominant control on the strain accommodation mechanism.

**Keywords:** GPS, Walker Lane, strain, kinematics, tectonics.

### INTRODUCTION

The Walker Lane belt is a structurally and kinematically complex zone of faulting in the Pacific–North America plate boundary zone between the Sierra Nevada Mountains and the Basin and

Range Province (Stewart, 1988; Wesnousky, 2005a) (Fig. 1). It accommodates about a quarter of the total Pacific–North America plate motion (Bennett et al., 2003; Oldow et al., 2001; Thatcher et al., 1999). Numerous studies of its active and recent tectonics have revealed that the system is characterized by many relatively short northwest-trending right-lateral faults, north-trending normal faults, and a smaller number of ENE-trending left-lateral

\*Corresponding author e-mail: Kreemer@unr.edu.

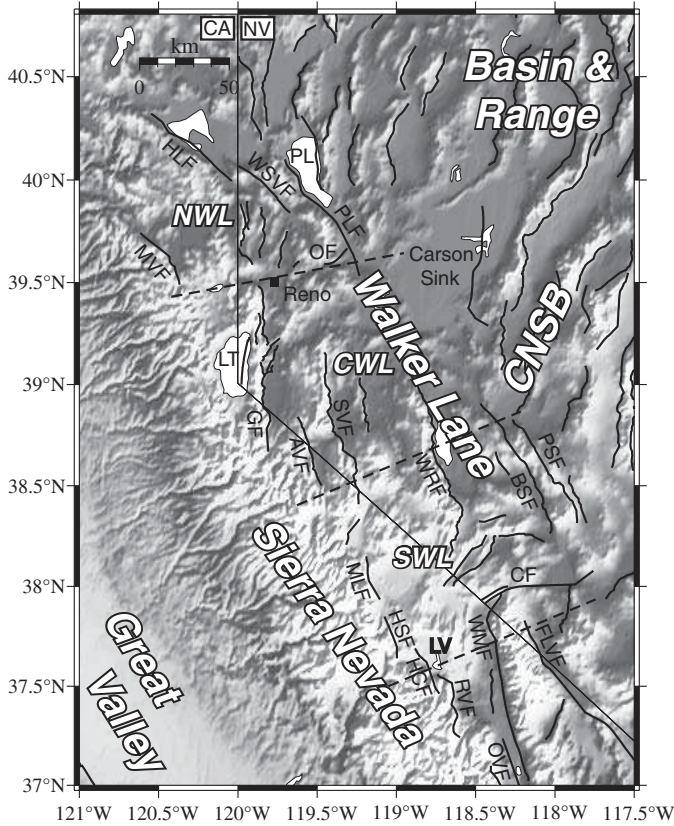


Figure 1. Overview map of the area of the main focus of this study. We divide the Walker Lane up into three segments: north (NWL), central (CWL), and south (SWL), separated by the dashed lines. AVF—Antelope Valley fault; BSF—Benton Springs fault; CA—California; CF—Coaldale fault; CNSB—Central Nevada seismic belt; FLVF—Fish Lake Valley fault; GF—Genoa fault; HCF—Hilton Creek fault; HLF—Honey Lake fault; HSF—Hartley Springs fault; LT—Lake Tahoe; LV—Long Valley; MLF—Mono Lake fault; MVF—Mohawk Valley fault; NV—Nevada; OF—Olinghouse fault; OVF—Owens Valley Fault; PL—Pyramid Lake; PLF—Pyramid Lake fault; PSF—Petrified Springs fault; RVF—Round Valley fault; SVF—Smith Valley fault; WMF—White Mountains fault; WRF—Wassuk Range fault; WSVF—Warm Springs Valley fault.

faults (Fig. 1) (e.g., Faulds et al., 2005b; Oldow, 2003; Slemmons et al., 1979; Stewart, 1988; Wesnousky, 2005a). It has been argued that the Walker Lane owes its tectonic complexity to (1) its location, i.e., it is situated between the approximately E–W–extending Basin and Range and the NW-moving Sierra Nevada–Great Valley microblock, (2) the fact that the current tectonic regime is geologically still young, and (3) the fact that many geologic features are inherited from pre-Walker Lane times. In general, it is now widely agreed upon that the Walker Lane is a young and developing transform or transtensional fault system (Faulds et al., 2005b; Wesnousky, 2005a, 2005b) characterized by the lack of long and well-developed faults, such as those present along, for example, the San Andreas fault system. At the latitude of  $\sim 39^\circ\text{N}$ , significant clockwise rotations around vertical axes have been observed by paleomagnetic measurements (Cashman and Fontaine, 2000). It

has been argued that the clockwise rotations and the presence of left-lateral (rotated) conjugate faults are consistent with having a partially detached elastic-brittle crust that is being transported on a continuously deforming substratum (Wesnousky, 2005a). The recent recognition of the Walker Lane as a developing transform zone has expanded our general understanding of the plate boundary-wide partitioning of Pacific–North America plate motion and the development of the plate-boundary zone in general.

Adding to the complexity is the Central Nevada seismic belt, a zone of focused historic earthquakes extending from the Walker Lane northeastward into the Basin and Range Province (Wallace, 1984) (Fig. 1). These earthquakes and the geodetic observation of relatively large strain rates localized at the Central Nevada seismic belt (Hammond and Thatcher, 2004; Thatcher et al., 1999) have led (in part) to the speculation that this belt plays an important role in the strain accommodation in the western Basin and Range Province (Wesnousky, 2005a; Wesnousky et al., 2005). However, the high geodetic strain rate is probably not a permanent feature, since it can be largely explained through viscoelastic postseismic strain relaxation (Hammond et al., this volume; Hetland and Hager, 2003). Moreover, the long-term significance of the Central Nevada seismic belt as a zone of localized deformation is not supported by some geologic studies of the slip history of the faults and the fault slip rates within the Central Nevada seismic belt relative to other Great Basin faults (Bell et al., 2004; e.g., Wallace, 1987), although the region appears to have a relatively high recurrence rate of surface-rupture earthquakes (Wesnousky et al., 2005). In the analysis that follows, we use the results of a companion paper (Hammond et al., this volume) to correct the geodetic strain rate field for transient postseismic effects that can disrupt the comparison between geodetically estimated strain and fault slip.

Geodetic velocity measurements, particularly using the global positioning system (GPS), allow for the precise quantification of crustal strain rates and provide constraints on regional present-day kinematics. Such measures provide important constraints for understanding the role of observed faulting and seismicity in the region. Knowledge of the present-day kinematic framework is also important in understanding finite-strain markers and the recent evolution of the deformation field. Several GPS studies have recently been undertaken in the Walker Lane region (Hammond and Thatcher, 2004; Oldow et al., 2001; Svarc et al., 2002b; Thatcher et al., 1999). These studies all found that deformation in the Walker Lane is characterized by relatively large strain rates, although they are not all consistent on how the strain rate is accommodated geologically. Oldow et al. (2001) inferred from their results that the central Walker Lane acts as a distributed zone of displacements linking the Eastern California shear zone with the northern Walker Lane and the Central Nevada seismic belts. They concluded as well that the relative displacements are not accommodated by a spatially smooth transition, but rather as differential motions of tectonic blocks. Svarc et al. (2002a) used their GPS velocity results to calculate a strain rate tensor for the Walker Lane at the latitude of Reno. They concluded that their

result is consistent with extension across and shear along a zone striking N35°W, which is the same orientation as the Pacific–North America small circle. Hammond and Thatcher (2004) obtained the same result, and, with Thatcher et al. (1999), found the strain rates in the Walker Lane to be significantly larger than elsewhere in the Great Basin, indicating to them that it is likely a zone of lithospheric weakness. Most of the geodetic results have illustrated the discrepancy that exists between geodetic deformation rates and those inferred from the slip activity of Quaternary faults (Hammond et al., this volume; Pancha et al., 2006). There are various explanations for that discrepancy, but the fact that the Walker Lane does not seem to behave as a mature fault system may provide a significant explanation.

In this study, we quantify the distributed strain rate tensor field in the Walker Lane region, taken here to be between ~37.5°N in the south and ~40.5°N in the north. For the purpose of this paper, we divide this part of the Walker Lane into three segments: a southern part south of ~38.75°N, a central part between 38.75°N and 39.5°N, and a northern part north of 39.5°N (Fig. 1). We address how faulting and other geologic and seismologic observations can be understood in terms of distributed strain. This is one of the first attempts to perform such analysis systematically along the entire Walker Lane. Because of the apparently diffuse nature of the deformation field, it is appropriate to analyze the deformation field in Walker Lane through modeling of the velocity gradient tensor field. From this, we can directly infer a continuous strain rate tensor field and interpolated velocities, as well as vertical-axis rotations. To do so, we combined published and updated GPS velocities into a synthesized observed velocity field, which has a much higher spatial resolution than similar previous attempts (Bennett et al., 2003; Oldow, 2003). To properly discuss and understand the context of contemporary deformation in the Walker Lane region, and to avoid modeling boundary effects, we briefly show and discuss our model results for the entire Great Basin region as well.

## VELOCITY VECTOR SYNTHESIS

To perform the strain rate analysis, we required a spatially dense set of geodetic velocities estimates. Therefore, we synthesized and combined the velocities of several independent studies into one consistent reference frame. Within the Great Basin proper, we used campaign-style GPS velocities from published studies (Hammond and Thatcher, 2004, 2005, 2007; McClusky et al., 2001; Oldow et al., 2001; Svarc et al., 2002b), the Southern California Earthquake Center (SCEC) v. 3 velocity solution (which includes some velocities derived from the very long baseline interferometry (VLBI) technique; Shen et al., 2003), continuous GPS (CGPS) velocity estimates from the University of Utah’s Eastern Basin and Range and Yellowstone Network (EBRY) (R. Smith, 2005, personal commun.), and U.S. Geological Society (USGS) campaign measurement results for the “Yucca Profile” (originally published by Gan et al. [2000], but we use a more recent solution from the USGS Web site). Crucial to providing a

robust regional frame, we include a CGPS velocity solution for the Basin and Range Geodetic Network (BARGEN) (e.g., Bennett et al., 1998, 2003) analyzed using the method of Blewitt et al. (this volume). Importantly, the permanent BARGEN network employs braced, deep, anchored monuments (down to ~10 m) into bedrock to ensure local stability (Langbein et al., 1995). We analyzed BARGEN data from 2000 to 2005.5, during which the GPS antenna/radome configuration was identical at each station (Smith et al., 2004). In addition, we include some vectors on the periphery of the Great Basin (including most of California’s Central Valley) (d’Alessio et al., 2005; Freymueller et al., 1999; Mazzotti et al., 2003; Svarc et al., 2002a; Williams et al., 2006). The Bay Area Velocity Unification (BAVU) solution of d’Alessio et al. (2005) includes a large number of USGS campaign results as well as velocities from the Bay Area Regional Deformation (BARD) continuous GPS network. Our data set includes all available velocities prior to September 2005.

To include each set of velocities into this compilation, we estimated and applied a six-parameter Helmert transformation using the horizontal velocities at collocated sites between studies. In theory, the transformation involves a three-parameter translation rate and a three-parameter rotation rate. However, when the collocated sites are geographically close to one another, as is the case for most studies used here, there is a trade-off between the translation and rotation. We therefore only applied the translation if an F-test indicated that a translation in addition to a rotation would provide a statistically significant improvement to the velocity fit at the collocated sites compared to a case when only a rotation was applied. We used a global GPS velocity solution in the International Terrestrial Reference Frame (ITRF2000), known as GPSVEL (Holt et al., 2005; Kreemer et al., 2006)—a solution derived from a rigorous combination of International GNSS Service (IGS) solutions using the method of Davies and Blewitt (2000)—as the benchmark study into which we transformed the regional studies. Most velocity fields can only be transformed after others have been transformed so that the number of collocated sites is increased. All studies used and their transformation parameters are listed in Table 1. Next, to obtain velocities in a North American (NA) reference frame, we subtracted from the ITRF2000 velocities the values estimated from the NA-ITRF2000 angular velocity as defined by the Stable North America Reference Frame (SNARF) Working Group (Blewitt et al., 2005): the Euler pole of NA-ITRF2000 motion is 2.4°S, 83.6°W, 0.2° m.y.<sup>-1</sup>. All 474 velocities (for 444 sites) in our study areas are shown in Figure 1 relative to the SNARF reference frame, and they are tabulated in a companion paper (Hammond et al., this volume).

To avoid spurious local strain rate anomalies, we discarded a small portion of GPS velocities that were significantly different from other nearby velocity estimates and that stood out from the regional pattern of velocity gradients. Often these anomalous velocities were from campaign-style measurements that only had measurements in two campaigns. Also, for some studies, we increased standard errors to be greater than those originally published (Table 1). Formal errors that are very small, particularly

TABLE 1. HELMERT TRANSFORMATION PARAMETERS

Study	$k$	Original ref.	$\omega_x$ ( $^{\circ}$ m.y. $^{-1}$ )	$\omega_y$ ( $^{\circ}$ m.y. $^{-1}$ )	$\omega_z$ ( $^{\circ}$ m.y. $^{-1}$ )	$\delta_x$ (mm yr $^{-1}$ )	$\delta_y$ (mm yr $^{-1}$ )	$\delta_z$ (mm yr $^{-1}$ )
BARGEN (this study)	2	ITRF00	-0.0141 $\pm$ 0.0381	-0.0490 $\pm$ 0.0909	0.0555 $\pm$ 0.0821	—	—	—
SCEC v. 3 (Shen et al., 2003)	1	N. Amer	0.0537 $\pm$ 0.0386	-0.1706 $\pm$ 0.0295	-0.0015 $\pm$ 0.0238	-2.60 $\pm$ 4.12	1.65 $\pm$ 3.44	3.56 $\pm$ 2.72
EBRY (R. Smith, 2005, personal commun.)	10	N. Amer	0.0198 $\pm$ 0.0019	-0.1988 $\pm$ 0.0043	-0.0125 $\pm$ 0.0042	—	—	—
Yucca profile	2	ITRF00	-0.0180 $\pm$ 0.1244	0.0031 $\pm$ 0.2399	0.0112 $\pm$ 0.1994	—	—	—
d'Alessio et al. (2005) (BAVU)	1	ITRF00	0.0061 $\pm$ 0.0009	0.0240 $\pm$ 0.0009	-0.0003 $\pm$ 0.0010	-1.41 $\pm$ 0.11	0.21 $\pm$ 0.11	1.82 $\pm$ 0.09
Freymueller et al. (1999)	1	Pacific	-0.3134 $\pm$ 0.1883	0.0022 $\pm$ 0.2988	-0.2924 $\pm$ 0.2918	—	—	—
Hammond and Thatcher (2004)	1	N. Amer	-0.0023 $\pm$ 0.0272	-0.2186 $\pm$ 0.0517	0.0211 $\pm$ 0.0482	—	—	—
Hammond and Thatcher (2005)	1	N. Amer	0.0173 $\pm$ 0.0285	-0.1847 $\pm$ 0.0525	-0.0138 $\pm$ 0.0519	—	—	—
Hammond and Thatcher (2007)	1	N. Amer	0.0303 $\pm$ 0.0143	-0.1894 $\pm$ 0.0278	-0.0113 $\pm$ 0.0258	—	—	—
Mazzotti et al. (2003)	1	ITRF00	0.0083 $\pm$ 0.0139	0.0247 $\pm$ 0.0233	-0.0157 $\pm$ 0.0309	—	—	—
McClusky et al. (2001)	2	N. Amer	0.0651 $\pm$ 0.0666	-0.0702 $\pm$ 0.1277	-0.1279 $\pm$ 0.1046	—	—	—
Oldow et al. (2001)	20	N. Amer	-0.0200 $\pm$ 0.2685	-0.2768 $\pm$ 0.4955	0.0488 $\pm$ 0.4559	—	—	—
Svarc et al. (2002a)	2	N. Amer	0.0588 $\pm$ 0.0890	-0.1289 $\pm$ 0.1572	-0.0669 $\pm$ 0.1506	—	—	—
Svarc et al. (2002b)	1	N. Amer	0.0093 $\pm$ 0.0616	-0.1667 $\pm$ 0.0970	-0.0468 $\pm$ 0.1103	—	—	—
Williams et al. (2006)	1	ITRF97	-0.0152 $\pm$ 0.0027	0.0271 $\pm$ 0.0053	-0.0349 $\pm$ 0.0055	—	—	—

Note: Cartesian components of the angular velocity ( $\omega_x$ ,  $\omega_y$ ,  $\omega_z$ ) and translation rate ( $\delta_x$ ,  $\delta_y$ ,  $\delta_z$ ) were solved for and applied to transform the velocities of each geodetic study from the original reference frame (Original ref.) into our ITRF2000 frame. The translation rate is only shown, and applied, when the transformation with translation led to a significantly better transformation compared to the case when only a rotation was applied (see text).  $k$ —factor with which the originally published formal velocity uncertainties are multiplied for use in our study. BARGEN—Basin and Range Geodetic Network; SCEC—Southern California Earthquake Center; EBRY—University of Utah's Eastern Basin and Range and Yellowstone Network.

with respect to those of nearby velocities, could lead locally to an overfit between the model and observed velocity, which in turn could potentially lead to locally spurious strain rate estimates.

## STRAIN RATE ANALYSIS APPROACH

In this study, we characterize the regional deformation field on the assumption that most of the crust in the Great Basin deforms in a spatially continuous fashion. Given the geodetic data, which indicate a smooth velocity gradient (Fig. 2), likely as the result of elastic strain accumulation on nearby locked faults, a continuous modeling approach is appropriate. Moreover, although in the long-term, the velocity gradient is accommodated as discrete steps across faults, the large number of faults justifies a continuous approach, and the long-term and observed large-scale strain field are not expected to be significantly different. To derive a continuous velocity gradient tensor field, we applied a spline interpolation technique (e.g., Haines and Holt, 1993; Holt et al., 2000). In this method, model velocities are fitted to the observed geodetic

velocities in a least-squares sense, using the full data covariance matrix. Model velocities are then interpolated using bicubic Bessel spline functions to derive a continuous velocity gradient tensor field, which provides estimates of strain rate, interpolated velocity, and vertical-axis rotation for any point in our model grid. Other studies using a similar model technique have been applied for the Pacific–North America plate-boundary zone (including most of the Basin and Range Province) using Quaternary faulting data, earthquake moment tensors, and early geodetic data (Flesch et al., 2000; Shen-Tu et al., 1998, 1999). However, the model resolution of those studies was limited by the use of relatively large grid cells in the inversion. Here, we use grid cells of  $0.2^{\circ} \times 0.2^{\circ}$ , which allow us to take advantage of the spatially dense velocity data that are now available in order to quantify the velocity gradients in higher detail than was previously possible.

We set up our model grid such that its northeastern edge is east of the Wasatch fault. No significant tectonic deformation appears to be present east of the Wasatch fault, as evidenced by the absence of Quaternary faults, seismicity, and insignificant

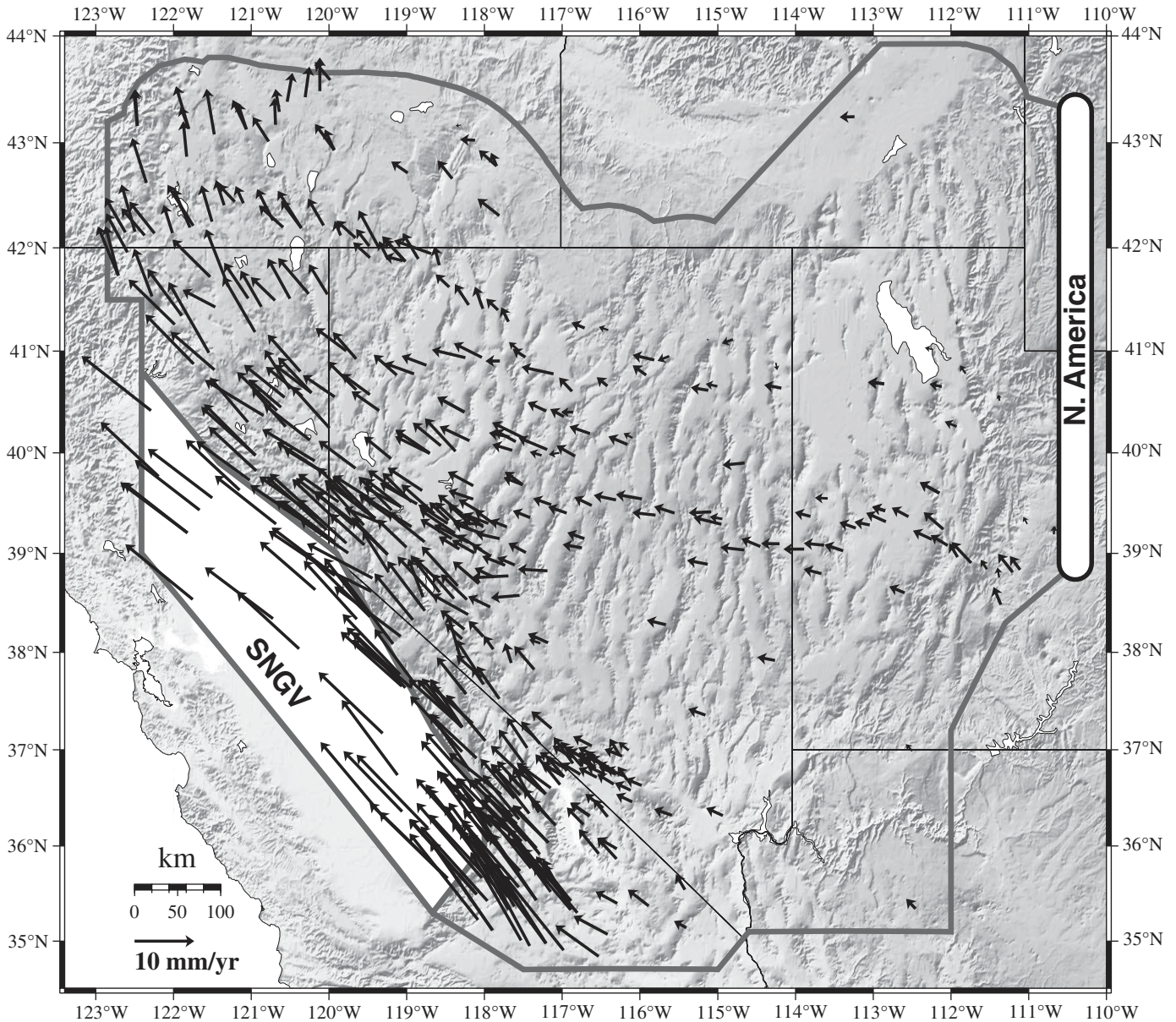


Figure 2. Geodetic velocities within the greater Great Basin, outlined by thick gray line. A  $0.2^\circ \times 0.2^\circ$  model grid is defined for our study area, with part of the grid defined a priori as the rigid Sierra Nevada–Great Valley block (SNGV, shown in white), and the eastern edge of the grid defined as North America. The geodetic velocities were compiled from multiple studies and are all shown in the same North America reference frame. Velocity uncertainties are omitted for clarity. In this figure, the correction for postseismic effects has not been applied.

GPS velocities of the easternmost sites in SNARF. Thus, we constrain the northeastern grid boundary to be equal to stable North America (Fig. 1). That is, we treat the velocities in our synthesized data set, which is in the NA reference frame, as being relative to this grid boundary. The southeastern edge of our model grid is near the western boundary of the Colorado Plateau (e.g., Bennett et al., 2003) and is free to deform, as is the northern grid boundary. The treatment of the western grid boundary is important to our analysis. We will present two models, one in which the Sierra Nevada–Great Valley is allowed to deform (the white

area in Fig. 2), and another where the Sierra Nevada–Great Valley moves as a rigid entity. Sierra Nevada–Great Valley motion is imposed as a rigid body rotation, which is estimated from the geodetic velocities, as discussed in the next section.

#### KINEMATIC BOUNDARY CONDITIONS

Rigidity and motion of the Sierra Nevada–Great Valley has been demonstrated by others (Argus and Gordon, 1991, 2001; Bennett et al., 2003; Dixon et al., 2000), and its motion provides

TABLE 2. ANGULAR VELOCITIES

	$\omega_x$	$\pm$	$\omega_y$	$\pm$	$\omega_z$	$\pm$	Pole lat. ( $^\circ$ )	Pole long. ( $^\circ$ )	$\omega$
	( $^\circ$ m.y. $^{-1}$ )		( $^\circ$ m.y. $^{-1}$ )		( $^\circ$ m.y. $^{-1}$ )				( $^\circ$ m.y. $^{-1}$ )
SNGV-SNARF	-0.1469	0.0184	-0.0874	0.0311	-0.0025	0.0286	-0.9	-149.3	0.171
CGB-SNARF	-0.0001	0.0152	0.0148	0.0322	-0.0430	0.0292	-71.1	90.4	0.045
SNGV-CGB	-0.1468	0.0184	-0.1022	0.0311	0.0405	0.0286	12.6	-145.2	0.183

*Note:* SNGV—Sierra Nevada–Great Valley block; CGB—Central Great Basin; SNARF—Stable North America Reference Frame. Sites used to estimate SNGV motion: 0306, 0605, 0607, 0609, 0611, 0614, 1008, 3188, A300, CHO1, CMBB, CNDR, H112, ISLK, JAST, KMED, LUMP, MINS, MUSB, LIND, ORLA, ORVB, SUTB, UCD1, UU83. Sites used to estimate CGB motion: ALAM, ECHO, EGAN, ELKO, FOOT, GOSH, MINE, MONI, RAIL, RUBY.

the most important kinematic boundary condition to constrain and understand Walker Lane deformation. For the strain rate model that imposes Sierra Nevada–Great Valley motion, we estimated the angular velocity based on 25 velocities that are within the region that we define as being Sierra Nevada–Great Valley (Fig. 2; Table 2). We will show later that having the eastern margin of the Sierra Nevada–Great Valley closely follow the Sierra Nevada crest is in general agreement with the available geodetic velocities in the high Sierras. The estimated Sierra Nevada–Great Valley angular velocity (relative to SNARF) is somewhat sensitive to the choice of the velocities to use in the estimation, but resulting angular velocity differences are insignificant for the purposes of this paper.

The central Great Basin, which lies to the east of the Walker Lane, has been shown to behave as a geodetically rigid microblock (Bennett et al., 2003; Hammond and Thatcher, 2005). Our strain rate modeling results indicate  $\sim 4$  nanostrain  $\text{yr}^{-1}$  for the central Great Basin (Fig. 3), the same order of magnitude as found for tectonic plates (e.g., Ward, 1998). Because later we would like to present our Walker Lane modeling results appropriately in an oblique Mercator projection around a Sierra Nevada–Great Valley–central Great Basin pole of rotation, we also estimate a central Great Basin–SNARF angular velocity based on 10 BARGEN sites (Table 2). We then combine that result with the Sierra Nevada–Great Valley (relative to SNARF) estimate to obtain the Sierra Nevada–Great Valley–central Great Basin angular velocity.

## RESULTS

### Great Basin

Before presenting our results for the Walker Lane, we briefly present the model strain rate field for the Great Basin as it is inferred directly from the geodetic velocity observations. Figure 3 shows the model velocity field and the contours of the second invariant of the model strain rates for a model that imposes rigid Sierra Nevada–Great Valley rotation. Formal uncertainties of the second invariant are on the order of 4–8 nanostrain  $\text{yr}^{-1}$ . As mentioned already, the central Great Basin shows very low strain rates and essentially moves as a geodetic microplate. Geologic strain rate estimates of  $\sim 1$  nanostrain  $\text{yr}^{-1}$  corroborate the geodetic results, but Wesnousky et al. (2005) pointed out that the

uncertainty in the geologic estimate is possibly large, and, along with Bennett et al. (2003), they asserted that prevalent Quaternary faulting in the central Great Basin precludes the notion of a long-lived rigid “microplate.” Strain rates are elevated east and west of the central Great Basin. The broad zone of elevated model strain rates in north-central Utah is at odds with studies that argued for localized strain along the Wasatch fault (Hammond and Thatcher, 2004; Martinez et al., 1998; Thatcher et al., 1999). However, a wide zone of elevated strain rate is consistent with an equally wide late Quaternary deformation field, derived from paleoseismic and seismic reflection data (Niemi et al., 2004), or the argument that the Wasatch fault is very late in the earthquake cycle (Malservisi et al., 2003). We show in a companion paper (Hammond et al., this volume) that the relatively high strain rates along the Central Nevada seismic belt are largely due to viscoelastic postseismic relaxation.

In the Eastern California shear zone and Walker Lane, strain rates are large as a consequence of the rapid east-to-west increase in velocity (as well as an  $\sim 20^\circ$  clockwise change in direction). Strain rates along the Eastern California shear zone are  $\sim 30$ – $130$  nanostrain  $\text{yr}^{-1}$ , and are  $\sim 30$ – $70$  nanostrain  $\text{yr}^{-1}$  in the Walker Lane, slightly larger than the average strain rates inferred by Bennett et al. (2003). Our strain rates estimates for the area near Reno, Nevada, are also somewhat larger than those found by Svarc et al. (2002a), but they are consistent with the results of Hammond and Thatcher (2004). Contrary to Bennett et al. (2003), our solution does not indicate lower strain rates for the central Walker Lane compared to the northern and southern parts. This discrepancy cannot entirely be explained by having, for this model, Sierra Nevada–Great Valley block motion as a boundary condition.

### Walker Lane

We show our results for the Walker Lane in Figure 4. Figure 4A contains the GPS velocities relative to Sierra Nevada–Great Valley. Figures 4B and 4C show the model velocities and principal strain rate axes (averaged for each grid cell) for a model that assumes a rigid Sierra Nevada–Great Valley and has Sierra Nevada–Great Valley–Stable North America Reference Frame motion applied as a boundary condition. Figure 4D shows the strain rate model for a case where the Sierra Nevada–Great Valley is part of the deforming grid, and no velocity boundary condition has been imposed. The strain results are corrected for the

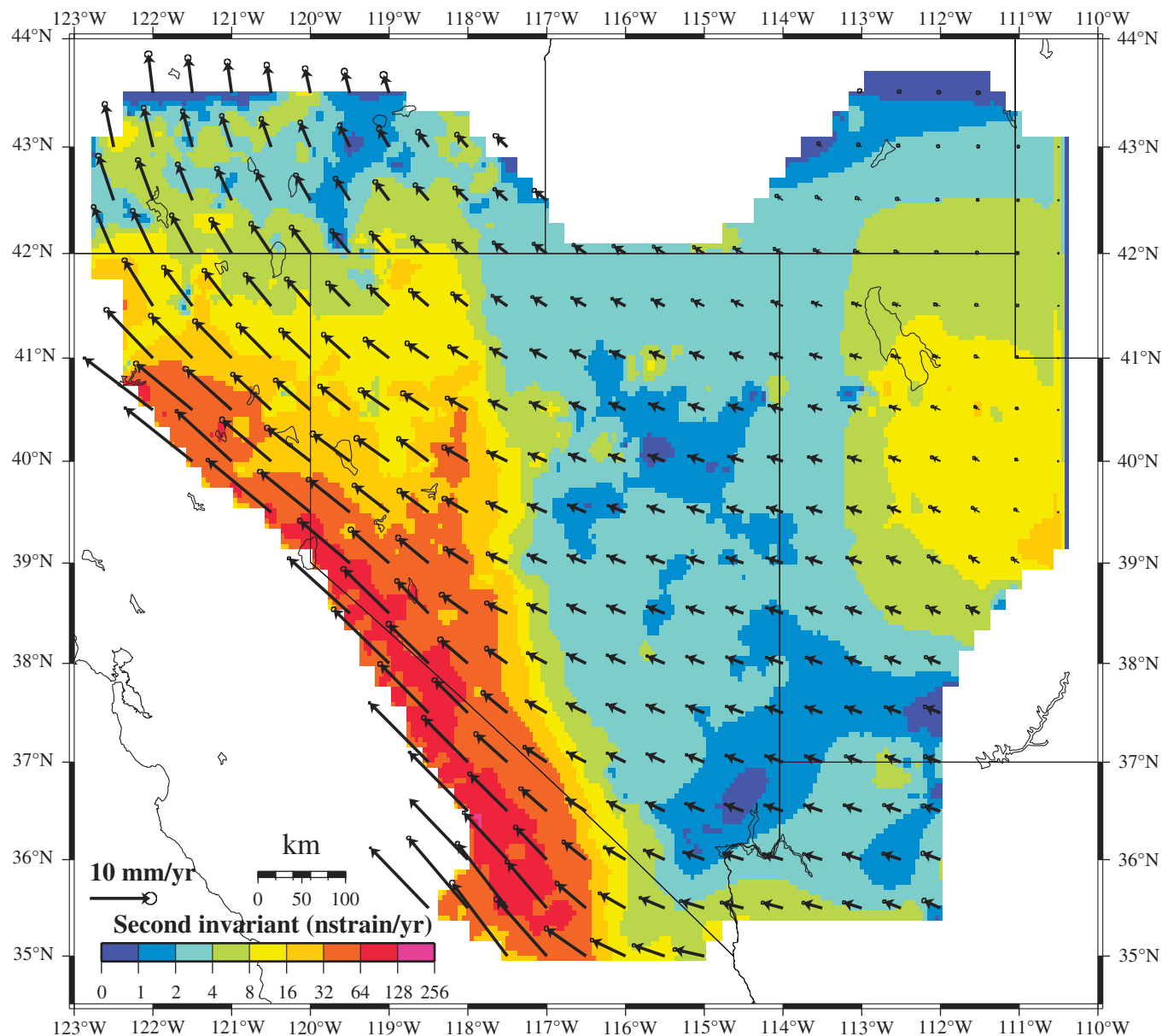


Figure 3. Color contour plot of second invariant of model strain rate tensor. Also shown are model velocities plotted at a regular grid relative to North America. Error ellipses represent one standard deviation.

effect of postseismic relaxation along the Central Nevada seismic belt (Hammond et al., this volume). To enhance interpretation of our results, we show the data results in an oblique Mercator projection with our Sierra Nevada–Great Valley–central Great Basin Euler pole (Table 2) as the pole of projection, and velocities are shown relative to our Sierra Nevada–Great Valley block. In this projection, any vector or feature aligned with the map’s up-down direction is along the Sierra Nevada–Great Valley–central Great Basin small circle.

The azimuths of the GPS velocities (Fig. 4A) show some variation from the small circle orientation, but, on average,

observed velocities are aligned along the small circles associated with Sierra Nevada–Great Valley–central Great Basin motion. However, a slight clockwise rotation can be seen, particularly in the interpolated velocity field (Fig. 4B), and its effect is most profound north of 40°N. This rotation probably results from the fact that the figure is in an oblique projection around the Sierra Nevada–Great Valley–central Great Basin pole, while for the most northern Walker Lane region, the central Great Basin does not properly provide the appropriate bounding block (Hammond and Thatcher, 2005). The model velocity field is very consistent with the BARGEN velocities (white vectors in Fig. 4A), which

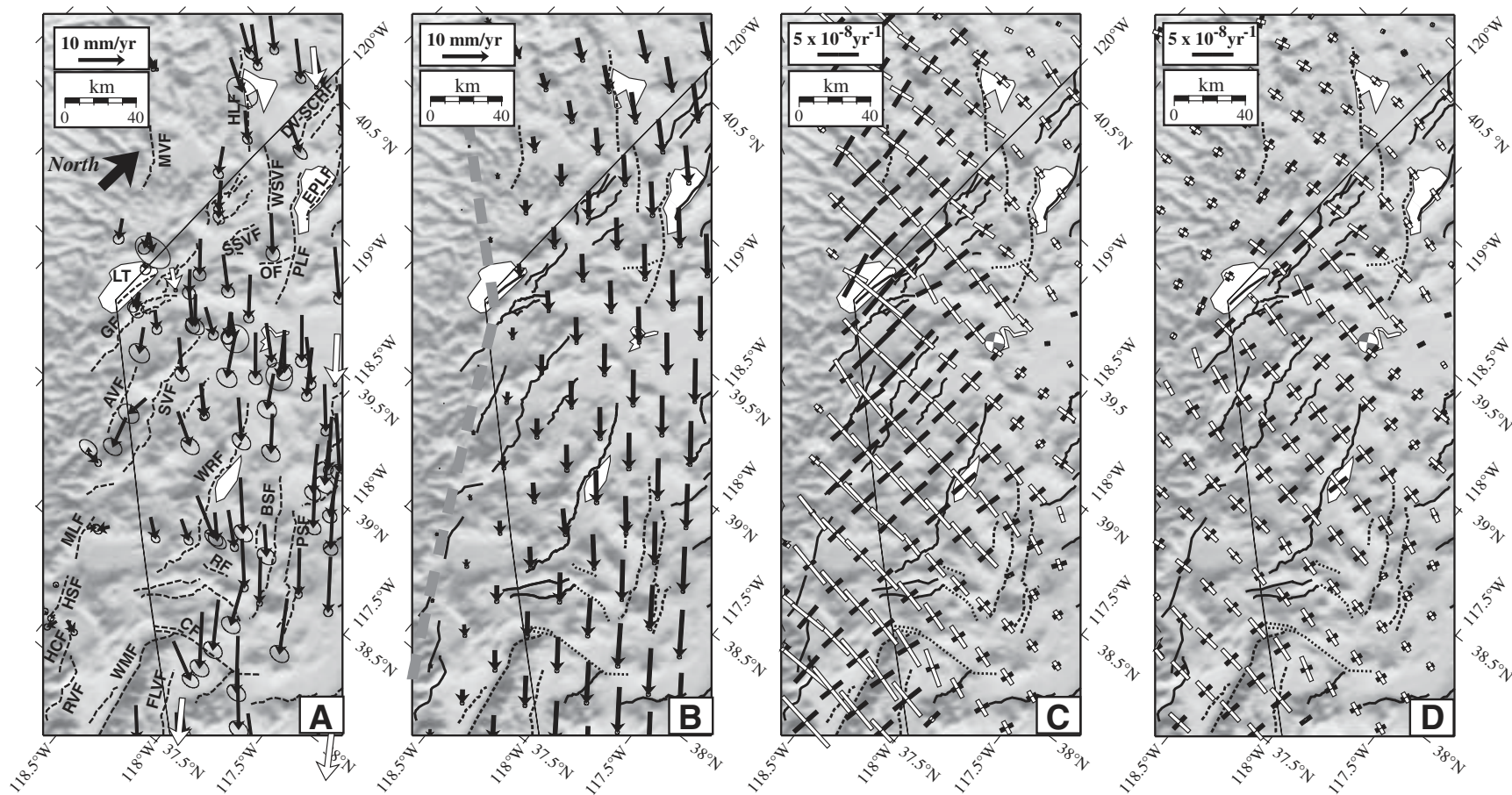


Figure 4. Oblique Mercator projection of the Walker Lane with the pole of projection equal to our obtained Sierra Nevada–Great Valley–central Great Basin Euler pole. (A) Global positioning system (GPS) velocities relative to the Sierra Nevada–Great Valley block that have been corrected for postseismic transient effects (white vectors for continuous BARGEN network, and black for all others). Error ellipses represent one standard deviation. Dashed lines are active faults: AVF—Antelope Valley fault; BSF—Benton Springs fault; CF—Coaldale fault; DV-SCRF—Dry Valley–Smoke Creek Ranch fault; EPLF—Eastern Pyramid Lake fault; FLVF—Fish Lake Valley fault; GF—Genoa fault; HCF—Hilton Creek fault; HLF—Honey Lake fault; HSF—Hartley Springs fault; LT—Lake Tahoe; MLF—Mono Lake fault; MVF—Mohawk Valley fault; OF—Olinghouse fault; PLF—Pyramid Lake fault; PSF—Petrified Springs fault; RF—Rattlesnake fault; RVF—Round Valley fault; SSVF—Spanish Springs Valley fault; SVF—Smith Valley fault; WMF—White Mountains fault; WRF—Wassuk Range fault; WSVF—Warm Springs Valley fault. (B) Model velocities relative to the Sierra Nevada–Great Valley block. Thick dashed line is eastern edge of our defined rigid Sierra Nevada–Great Valley block. Continuous black lines are normal faults, dashed lines are (dominantly) right-lateral faults, and dotted lines are (dominantly) left-lateral faults. (C) Principal model strain rate axes. White and black bars are extensional and contractional strain rate axes, respectively. Faults are indicated similarly as in B. Focal mechanism in western Carson Sink is for a 1992  $M_w = 4.1$  event (Ichinose et al., 2003). (D) Same as C, except for this model rigid motion of the Sierra Nevada–Great Valley block is not imposed as a velocity boundary condition.

provide strong constraints on our model solution because of their relatively small uncertainty. Despite the CGPS strong constraints, there are only a few CGPS velocities, and the campaign-style velocity measurements provide essential data in refining and confirming the deformation pattern implied by the CGPS velocities. Our results show that for the model with a rigid Sierra Nevada–Great Valley constraint,  $\sim 10 \text{ mm yr}^{-1}$  is accommodated over a distance of  $\sim 135 \text{ km}$  across the Walker Lane, and the width of this shear zone is roughly constant from north to south. Motion of  $10 \text{ mm yr}^{-1}$  of the eastern Walker Lane relative to the Sierra Nevada–Great Valley block is smaller than the earlier estimate by Thatcher et al. (1999), but it is in agreement with more recent estimates (Bennett et al., 2003; Hammond and Thatcher, 2004, 2007). Our results are different from Bennett et al. (2003) in that they found the width and total motion across the Walker Lane to vary along the Walker Lane, and we do not find that. The reasons for this difference can likely be found in the fact that we corrected for the effect of postseismic relaxation and in our treatment of the Sierra Nevada.

There is a significant difference between the strain magnitudes between the models with and without an imposed rigid Sierra Nevada–Great Valley (Fig. 4C vs. 4D). The difference in style of the tensor field is minimal. Without the assumption of a rigid Sierra Nevada–Great Valley, the model predicts significant strain rates in the Sierra Nevada and, in relation, lower strain rates in Walker Lane closest to the Sierra Nevada. Strain rate values toward the Basin and Range Province are roughly identical between the two models. For the most part, the difference in strain fields is the result of a lack of GPS velocity observations in the Sierra Nevada (particularly north of  $\sim 39^\circ\text{N}$ ), which causes a wide velocity gradient between the Walker Lane and the Great Valley. A secondary, and minor, reason for the difference is that the model results involves some level of smoothing, causing strain rates to diffuse into the Sierra Nevada in the case when the Sierras are not modeled as behaving rigidly.

The general alignment of the velocities with the small-circle orientation indicates that the deformation field is dominated by shear as a result of Sierra Nevada–Great Valley–central Great Basin motion. This is emphasized by the strain rate tensors, which generally have principal contractional and extensional strain rate axes of equal length, indicating shear (Figs. 4C–4D). The data and model results point out several general features of the kinematics in the Walker Lane. In the north (i.e., north of Lake Tahoe), shearing along the Sierra Nevada–Great Valley–central Great Basin small-circle direction dominates in the west, while smaller, dominantly extension, strain rates are present in the vicinity of Pyramid Lake. The Honey Lake (HL), Warm Springs Valley (WSV), Pyramid Lake (PL), and Mohawk Valley (MV) faults are optimally oriented to accommodate the inferred  $\sim 10 \text{ mm yr}^{-1}$  total right lateral motion across these faults. Similarly, the Dry Valley–Smoke Creek Ranch, Eastern Pyramid Lake, and Spanish Springs Valley faults are well oriented to accommodate the extensional component of the strain tensor, and they are also consistent with the focal mechanisms of several earthquakes in

this area (Ichinose et al., 2003). Our model result shows that the region around Pyramid Lake is predominantly extending (Fig. 3C). Although this would agree with extension across the East Pyramid Lake and Spanish Springs Valley normal faults, it contradicts the geological findings that displacements in the region are predominantly right-lateral (Briggs and Wesnousky, 2004; Faulds et al., 2005b). We argue that this discrepancy may be an artifact of an insufficient number of reliable GPS velocities east of the Warm Springs Valley and Pyramid Lake faults.

South of the latitude of Lake Tahoe, the model strain rates indicate predominant shear, but the extensional strain component increases from the north to the south. The orientations of right-lateral faults, such as Fish Lake Valley, Petrified Springs (PS), and Benton Springs (BS) faults, are roughly along the small-circle orientation, indicating that they are well oriented to accommodate part of the  $10 \text{ mm yr}^{-1}$  of shear. Most other faults are oblique to the shear direction. In the central Walker Lane, the extensional component of the strain tensor is oriented consistently with the observed normal slip activity along normal faults such as the Genoa, Smith Valley, and Wassuk Range faults (e.g., Ramelli et al., 1999; Surpluss et al., 2002). Our model results are not conclusive concerning the strain tensor style and orientation for Sierra range–bounding faults, such the Mono Lake and Hartley Springs faults, where the effect of choice of boundary condition is most profound. Further south, the strain tensor is more transtensional in style, and the orientation of the extensional axis deviates more from being perpendicular to faults such as, for example, the White Mountains (WM) fault. The latter is consistent with the observation that the White Mountains fault has accommodated oblique slip since ca. 3 Ma (Stockli et al., 2003; Wesnousky, 2005a). The strain rate tensors near the Rattlesnake and Coaldale faults are consistent with their behavior as left-lateral conjugate faults (with an extensional component) within a regional-scale right-lateral shear zone (Wesnousky, 2005a).

## DISCUSSION

### Transtension

The large-scale kinematics of the northern Walker Lane, as quantified by our strain rate model, the orientation of Sierra Nevada–Great Valley fixed velocities, and fault orientations and styles, are largely controlled by Sierra Nevada–Great Valley motion with respect to the Basin and Range Province. An earlier analysis of faulting along the entire eastern margin of the Sierra Nevada–Great Valley block came to the same conclusion (Unruh et al., 2003). Like Unruh et al. (2003), we find that the deformation field is not entirely characterized by simple shear strain, but rather by transtension. We note, however, that we observe transtension primarily south of  $39^\circ\text{N}$ . The transition from shear-dominated strain rates north of  $39^\circ\text{N}$  and transtension-dominated strain rate south of  $39^\circ\text{N}$  coincides with the change in the orientation of our defined eastern edge of the Sierra Nevada–Great Valley block. It could be argued that our transtensional strain rate results are

simply a reflection of our imposed boundary condition. However, we see roughly the same pattern when we do not impose Sierra Nevada–Great Valley rigid body rotation as a boundary condition (Fig. 4D). Other studies also remarked that the transtension south of 39°N is due to the fact that the velocity field does not parallel the orientation of the eastern margin of the Sierra Nevada–Great Valley block (Oldow, 2003; Unruh et al., 2003).

Our results do not indicate fault-normal extension along the Genoa fault and within the Lake Tahoe basin. Yet, the orientations and locations of these faults, as well as the Quaternary faulting history along the Genoa fault (Ramelli et al., 1999), geophysical imaging (Kent et al., 2005), and Holocene seismic activity (Schweickert et al., 2004) near Lake Tahoe all indicate that these are, to first order, Sierra range–bounding normal faults. Moreover, the hypothesized lower crustal magma intrusion underneath Lake Tahoe in 2003 is consistent with crustal extension in a roughly E–W direction (Smith et al., 2004). Those observations would be consistent with the strain rate results if we would have imposed the eastern Sierra Nevada–Great Valley boundary to cut Lake Tahoe from south to north and then continue onward along the Mohawk Valley fault. Such geometry would create a large releasing bend across Lake Tahoe, with significant E–W extension across it. Unfortunately, the geodetic velocities northwest of Lake Tahoe that are available are rather unreliable kinematic indicators (Fig. 4A) and do not allow us to make conclusive inferences about the strain rate there and whether it could be considered part of the Sierra Nevada–Great Valley block. Tectonics near Lake Tahoe could be explained with having a large releasing bend in the eastern margin of the rigid Sierra Nevada–Great Valley block, but that does not reconcile the shear strain across normal faults such as the Smith Valley and Wassuk Range faults. If these faults play an important system role in the accommodation of the overall shear strain, then their simplest role would be of releasing or transfer steps between right-lateral faults. However such faults are not well documented. We discuss this in more detail in a section below.

### “The Rate Debate”

At many places along the Walker Lane, a discrepancy appears to exist between the required total strike-slip motion imposed by GPS and that inferred geologically. Compare, for instance, the plots of the geodetic strain rate (Fig. 3) and geologic strain rates (Fig. 2 of Hammond et al., this volume). A similar discrepancy is found for the Basin and Range Province as a whole (Pancha et al., 2006). Next, we present a short overview of the geodetic and geologic values, largely in a regional context, as our study does not attempt to infer slip rates on individual faults.

In the most northern Walker Lane, the total range of geologic strike-slip rates (for the combined Honey Lake, Warm Springs Valley, and Pyramid Lake faults) is ~2–10 mm yr<sup>-1</sup> (Faulds et al., 2005b). When adding a considerable, but still yet unknown, slip rate for the Mohawk Valley fault, the geologic rate is roughly consistent with the total geodetic rate of ~10 mm yr<sup>-1</sup>. Ham-

mond and Thatcher (2007) used GPS campaign-style velocities (included in our velocities) to invert for fault slip rates and concluded that a preferred and maximum total of ~7 mm yr<sup>-1</sup> and ~9 mm yr<sup>-1</sup>, respectively, can be accounted for as right-lateral slip across the Mohawk Valley, Honey Lake, Warm Springs Valley, and Pyramid Lake faults.

Further south, in the central Walker Lane, no such consistency can be found. There, the dearth of significant observed Quaternary dextral strike-slip offsets (dePolo and Anderson, 2000) is puzzling. No right-lateral strike-slip fault is known to exist over a region ~100 km south of the Pyramid Lake fault. The only recognized significant strike-slip faults in the central Walker Lane, the Benton and Petrified Springs faults, have minimum slip rates of ~1 mm yr<sup>-1</sup> (Wesnousky, 2005a).

More south, in the southern Walker Lane, the relative geodetic motion is roughly consistent with the relatively high geologic rates inferred for the Fish Lake Valley (FLV) fault (Reheis and Sawyer, 1997), as concluded elsewhere as well (Dixon et al., 2003). Predicted relative motion of 2 mm yr<sup>-1</sup> over the White Mountains fault is higher than some observed geologic rates (dePolo, 1989; Reheis and Dixon, 1996) but more consistent with others (e.g., Schroeder et al., 2003).

The discrepancy between geologic and geodetic rates is most profound for the central Walker Lane. An outstanding question is: Does the discrepancy point to shortcomings or incompleteness in the paleoseismic slip estimation? The total cumulative slip on normal faults may approach the level of extension predicted as part of the inferred strain rate tensors. However, that would still require either a large amount of right-lateral slip between the normal faults on unknown strike-slip faults or a significant component of strike-slip motion on known normal faults. Does the discrepancy instead point to inappropriateness in the rate comparison? This would be the case, for instance, when a fault has a significant offset due to unrecognized aseismic slip, then the paleoseismic investigations are likely to underestimate the total offset. However, no documentation of “creeping” faults is available. Another case of an inappropriate comparison would be if only GPS velocities near a locked fault are considered, such that the full slip rate at depth may not be captured. However, most studies that have investigated the rate discrepancy consider slip rates over the entire Walker Lane belt or multiple faults, rather than one single fault, such that the geodetic velocity measurements should capture all of the interseismic strain. This leaves only one other explanation for the rate discrepancy: Can it be explained by strain accommodating processes other than slip along main faults? We investigate this third explanation below.

### How Is Deformation Accommodated?

#### *Right-Lateral Faulting*

The simplest explanation of how the dextral shear is accommodated in the central Walker Lane is that it is simply done through right-lateral strike-slip faulting on undiscovered structures. Although no through-going dextral fault cuts the surface of

the central Walker Lane between the Pyramid Lake and Benton Springs faults, some evidence of such a fault (zone) has recently emerged from field observations of possible dextral offsets and a topographic lineament in the western Carson Sink (J. Faulds, 2005, personal commun.). There is some additional evidence that NW-directed slip is currently being accommodated through strike-slip faulting. First, focal mechanism azimuths for the 1954 Fairview Peak and Rainbow Mountain earthquakes are  $\sim N30^\circ W$  (Doser, 1986), even though the surface breaks are oriented  $\sim N17^\circ E$  (Caskey et al., 2004). The slip direction of these events is close to the  $\sim N35^\circ W$  strike of the Benton Springs and Petrified Springs faults, which are located only  $\sim 25$  km southeast of the Rainbow Mountain rupture. The 1932 Cedar Mountain earthquake displayed a similar discrepancy between seismic slip and surface faulting, as was seen for the 1954 events (e.g., Bell et al., 1999), and this discrepancy has been explained as the expression of Riedel shears above a fault at depth (Bell et al., 1999; Caskey et al., 2004). Secondly, while there is a dearth of mapped faults in the Carson Sink, a hint of its tectonic activity was revealed there by an  $M_w = 4.1$  event in 1992 that had a strike-slip mechanism with one nodal plane trending  $N33^\circ W$  (Ichinose et al., 2003). Thirdly, based on oblique striae rakes on the Wassuk Range fault (Stewart, 1988), evidence of small pull-apart basins and oblique dextral slip along this fault (Surpless et al., 2002), and orientations and arguable offsets of minor faults northwest of the mapped trace of the Wassuk Range front, called the White Mountain fault (Bell, 1981; Bingler, 1978; Wesnousky, 2005a), this region shows some evidence of right-lateral offsets.

### Block Rotations

Crustal block rotation around a vertical axis, often involving “bookshelf faulting,” is a well-described process in a zone of distributed homogeneous shear (e.g., McKenzie and Jackson, 1983; Nur et al., 1988). Through rotation, a significant part, or all, of the velocity gradient tensor can be accommodated. This process is well described for, for instance, the southern San Andreas fault system (Nicholson et al., 1986) and the northeastern Mojave Desert (e.g., Garfunkel, 1974; Nur et al., 1988), and the latter was recently corroborated with GPS velocity measurements (Savage et al., 2004).

It has been argued that clockwise rotations within the central Walker Lane accommodate, and have accommodated, a significant portion of the overall right-lateral shear, particularly south of the Pyramid Lake fault (known as the Carson domain) and near the Excelsior mountains, between the Benton Springs fault and the White Mountains and Fish Lake Valley faults (Cashman and Fontaine, 2000; Wesnousky, 2005a). Observed paleomagnetic rotations (Cashman and Fontaine, 2000) and observed (e.g., Olinghouse, Rattlesnake, and Coaldale faults), and inferred (i.e., the Carson and Wabuska lineaments; Stewart, 1988), left-lateral faults (or lineaments) hint at such an explanation. In this case, the crustal blocks between the left-lateral faults and lineaments act as the “books” in a “bookshelf faulting” scenario with the Pyramid Lake, Benton Springs, and Petrified Springs faults as the east-

ern “shelf.” For this scenario, it is unclear what structures comprise the western “shelf.” For the Carson domain, paleomagnetic clockwise rotation rates since 9–13 Ma have been estimated at  $6 \pm 2^\circ \text{ m.y.}^{-1}$ , with some indication that rotation has been slowing down over time (Cashman and Fontaine, 2000).

If currently present, can we observe crustal block rotations geodetically? Over timescales that are large compared to the seismic cycle, blocks translate and rotate with episodic slip along the fault zones between them. However, when measured over short timescales, and when unaffected by earthquakes, geodetic velocities cannot directly detect individual motions of blocks with small dimensions, i.e., 10–50 km. This is not only because of elastic loading along the block’s bounding faults, but also because the lateral dimensions of the block under study are of the same order of magnitude as the elastic thickness of the block. As a consequence, the crust acts as a low-pass filter and geodetic velocities reflect only the strain accommodations over length scales many times the thickness of the crust. It is for these reasons, and the very low number of velocity measurements to be expected on any small crustal block, that we are cautious of studies that interpret geodetic velocities directly in terms of the kinematics of a small block, such as Oldow et al. (2001).

Even though geodetic velocities cannot directly constrain the rotation of small crustal blocks, we can infer from the velocity gradient model the contemporary rotation rate within the diffuse deformation zone, i.e., the vorticity of the velocity gradient tensor field, not a rigid block rotation. The relationship between these geodetic rotations and finite rotations is complicated because it is dependent on the size and orientations of crustal blocks (e.g., Lamb, 1994; McKenzie and Jackson, 1983). Nevertheless, we find relatively constant clockwise rotation rates of  $1\text{--}2^\circ \text{ m.y.}^{-1}$  for the Carson domain, and, regardless of the difficulties in comparing geodetic and finite rotations, we note that the geodetic rotation rate is significantly lower than the paleomagnetic estimates. Perhaps this is an expression of the deceleration of rotation since 9 Ma. If rotation is the only mechanism to accommodate the regional velocity gradient, a slowing down of rotation rate is surprising, because there is no indication that motion along the Walker Lane has slowed down since its inception at ca. 9 Ma. In fact, it has been argued that the Walker Lane is propagating northwestward as the Mendocino triple junction migrates northward along California’s coast (Faulds et al., 2005b), with less cumulative slip in the north compared to the south (e.g., Faulds et al., 2005a; Wesnousky, 2005a). Thus, for the central Walker Lane region, the mechanism of rotation may have possibly been more significant between 9 and 3 Ma, compared to present-day, when the area was located ahead or near the “tip” of the propagating shear zone. This would be consistent with the latest timing estimate of onset of faulting (ca. 10 Ma) along the strike-slip faults of the central Walker Lane (Hardyman and Oldow, 1991).

Such a process can be seen at present, for instance, in central Greece, where significant vertical-axis rotation contributes significantly to the strain accommodation required in front of the North Anatolian fault as it propagates toward the Gulf of

Corinth (e.g., Armijo et al., 1996; Clarke et al., 1998; Kissel and Laj, 1988). Once a through-going shear zone has developed, block rotation will become less significant over time, in favor of strike-slip faulting.

### **Central Nevada Seismic Belt**

It has been suggested that the Central Nevada seismic belt plays an important role in Walker Lane kinematics, transferring dextral shear (Faulds et al., 2005a; Oldow et al., 2001; Wesnousky et al., 2005) onto N-NE–striking normal faults. This idea has been based on several observations, but, most importantly, on the fact that earlier GPS velocity measurements suggested that the Central Nevada seismic belt separates  $\sim 6 \pm 2 \text{ mm yr}^{-1}$  of total motion across the northern Walker Lane and  $\sim 10 \text{ mm yr}^{-1}$  across the southern portion (Gan et al., 2000; Thatcher et al., 1999). This would be consistent with the decrease of total offset from the southern to northern portion of Walker Lane (Faulds et al., 2005a; Wesnousky, 2005a). We show here that the motion over the northern Walker Lane is very similar to the motion over central and southern Walker Lane, in particular, when the effect of postseismic deformation from the Central Nevada seismic belt earthquakes is removed from the regional deformation field. Hammond et al. (this volume) assumed that when the time-dependent deformation is removed, extension across the Central Nevada seismic belt would be  $\sim 1 \text{ mm/yr}$ , which is slightly elevated compared to the region further to the east. This is consistent with earthquake recurrence times being higher at the Central Nevada seismic belt than elsewhere in the central Great Basin (Wesnousky et al., 2005). Thus, although the twentieth-century seismicity along the Central Nevada seismic belt may have enhanced the apparent surface deformation, which could lead to an overemphasis of its role, the Central Nevada seismic belt likely plays some role in the regional strain accommodation. This idea is also supported by the orientation of the Central Nevada seismic belt relative to the Walker Lane trend and the fact that it connects to the Walker Lane where strike-slip faulting is not well established.

### **What Drives the Deformation?**

We find that the strain rate field for the Walker Lane is, to first order, rather simple: the width of the zone is roughly constant, the strain rate magnitude in the zone is roughly constant, and the style of strain rate is dominated by shear/transension throughout most of the region. The relative simplicity of the geodetic deformation field contrasts with the tectonic complexity inferred from the available (and, at places, lack of) geologic data discussed previously. Wesnousky (2005a) postulated that the complexity of faulting and the apparent rotation of crustal blocks are consistent with the concept of a partially detached elastic-brittle crust that is being transported on a continuously deforming anelastic substratum. Faulds et al. (2005a) noted that strike-slip faults in the northern Walker Lane appear to act as large-scale Riedel shears above a shear zone at depth. On physical arguments, it has been argued that the smoothness of the geodetic velocity field in a transform zone reflects the long-term continuous deformation in the lower

lithosphere (Bourne et al., 1998). Although Bourne et al. (1998) argued that the subcrustal shear zone drives the long-term movement of crustal blocks, similar to the floating block model of Lamb (1994), it should be noted that for a transform zone, the driving force of the instantaneous crustal deformation field is not uniquely resolvable from the geodetic velocity field and may come from the side or from beneath (Savage, 2000). Indeed, we observe that based on the orientation of the deformation zone, on the orientation of principal strain rate axes, and on the apparent influence of the geometry of the Sierra Nevada–Great Valley block on the Walker Lane strain rate tensor field, deformation in the Walker Lane is strongly controlled (and perhaps driven) by the Sierra Nevada–Great Valley block motion. Those strain features can be seen in Figures 4C and 4D, and our inference is thus not biased by whether or not we model the Sierra Nevada as a part of a rigid Sierra Nevada–Great Valley block.

### **Summary of Discussion**

Irrespective of the actual driving mechanism, the surface complexity of the Walker Lane tectonic system is an expression of either its relative youth compared to, for example, the San Andreas fault system (Wesnousky, 2005b), and/or the influence of inherited structure. There is some suggestion that the southern Walker Lane region is more mature than the northern Walker Lane. Total dextral displacements are 48–75 km in the south (Ekren and Byers, 1984; Oldow, 1992) and 20–30 km in the north (Faulds et al., 2005b), and the inception of strike-slip faulting has been documented at ca. 6 Ma along the Fish Lake Valley fault (Reheis and Sawyer, 1997) and could be as recent as ca. 3 Ma in the northern Walker Lane (Henry et al., 2007). We show here that the difference in amount of finite strain between the northern and southern portions of Walker Lane is not matched by differences in the contemporary strain rate field (as was suggested by earlier GPS results), and we argue that Sierra Nevada–Great Valley block motion is the dominant kinematic boundary condition along the length of the entire Walker Lane. The discrepancy between cumulative offset and present-day strain rate distribution raises a few questions. Why does the northern Walker Lane appear as a more mature shear zone compared to the central Walker Lane? The Honey Lake and Warm Springs Valley faults (or at least the basement fault underneath them) are reactivated normal faults (Henry et al., 2007), and this reactivation may have occurred because those faults are optimally oriented to accommodate the shear. The normal faults in the central Walker Lane are more oblique to the shear orientation, which would inhibit them to reactivate as strike-slip faults (perhaps with the exception of the most northern Wassuk Range fault). Moreover, the process of crustal block rotations may have accommodated most of the strain without the need for those normal faults to take up a strike-slip component. If the rate of crustal rotations has slowed down, as suggested by the findings of Cashman and Fontaine (2000), one would expect oblique or dextral slip to become more prevalent on the normal faults, as has been documented further

south along the White Mountains fault (Stockli et al., 2003), but concrete evidence for that is still missing.

Another point of consideration in understanding the discrepancy between finite strain and geodetic strain rate in the northern Walker Lane is that, kinematically, it is possible to have a shear zone with equal total displacement rates along its entire length that terminates rather abruptly. This can be seen, for example, in the northern Aegean, where the North Anatolian fault slips at a constant rate of  $\sim 24 \text{ mm yr}^{-1}$  up to its abrupt termination near the Gulf of Evvia (Kreemer et al., 2004). In order to accommodate the deformation in the region in front of the propagating fault tip, relatively large contemporary vertical-axis rotation rates are expected, and can be seen, together with graben opening, in central Greece (Armijo et al., 1996; Clarke et al., 1998; Goldsworthy et al., 2002). The observed crustal rotations in the central Walker Lane ahead of the more established shear zone south of  $38^\circ\text{N}$  may be analogous. However, we would then also expect to see relatively large contemporary rotation northwest of the Honey Lake fault, where no active strike-slip fault has been documented. Moreover, we would expect to see relatively high activity along normal faults north of the Honey Lake–Warm Springs Valley fault system. Such activity is not documented, but given that migration of zones of active faulting has been documented before (Wallace, 1987), a future Central Nevada seismic belt–like zone of activity may be to the northwest of the Central Nevada seismic belt, connecting to the Walker Lane near  $40.5^\circ\text{N}$ .

## CONCLUSIONS

We have presented a velocity and strain rate model for the northern part of the Walker Lane derived from a compilation of geodetic velocities. We find that the Walker Lane region from  $37.5^\circ\text{N}$  to  $40.5^\circ\text{N}$  is characterized by an  $\sim 135\text{-km}$ -wide zone with relatively constant strain rates associated with  $\sim 10 \text{ mm yr}^{-1}$  total motion across the zone. These findings are consistent with most recent geodetic studies, from which came much of the data used in this study. The strain rates depict predominantly strike-slip deformation, but south of  $39^\circ\text{N}$ , the extensional component of the strain rate tensor increases, reflecting a more transtensional domain there. This transtension is the consequence of the motion of the Sierra Nevada–Great Valley block not being parallel to its eastern margin, i.e., the eastern Sierra front, south of  $39^\circ\text{N}$ . While several main faults in the northern and southern Walker Lane are consistent with the strain rate model results, the geologic mode and rate of deformation in the central Walker Lane are less clear. Left-lateral faulting and clockwise rotations there may contribute to the accommodation of the velocity gradient tensor field, and most normal faults are optimally oriented to accommodate some component of the regional shear strain. However, significant additional dextral strike-slip faulting is required to accommodate the majority of the  $10 \text{ mm yr}^{-1}$  relative motion. Several observations point at the accommodation of dextral shear in the Carson Sink, but no consistent pattern has emerged yet. The geologic complexity and variation along the length of the Walker Lane are

in contrast with the relatively simple strain rate field. This suggests that (1) various mechanisms are at play to accommodate the shear, (2) parts of the surface tectonics may (still) be in an early stage of development, and (3) inherited structural grain can have a dominant control on the strain accommodation mechanism.

## ACKNOWLEDGMENTS

This research was funded in part by Department of Energy grant DE-FG36-02ID14311 to the Great Basin Center for Geothermal Energy and by the Department of Energy Yucca Mountain Project/Nevada System of Higher Education Cooperative Agreement DE-FC28-04RW12232. We thank D. Lavallée for providing his global velocity solution, T. Williams for providing us with his velocity solution before publication, R. Smith for making the unpublished results of the EBRY network available, and the U.S. Geological Survey for making all their campaign results publicly available. We thank J. Bell, S. Wesnousky, and J. Faulds for helpful discussions, and we are grateful to S. Wesnousky, P. LaFemina, and an anonymous reviewer for comments that improved this paper significantly.

## REFERENCES CITED

- Argus, D.F., and Gordon, R.G., 1991, Current Sierra Nevada–North America motion from very long baseline interferometry: Implications for the kinematics of the western United States: *Geology*, v. 19, p. 1085–1088, doi: 10.1130/0091-7613(1991)019<1085:CSNNAM>2.3.CO;2.
- Argus, D.F., and Gordon, R.G., 2001, Present tectonic motion across the Coast Ranges and San Andreas fault system in central California: *Geological Society of America Bulletin*, v. 113, p. 1580–1592, doi: 10.1130/0016-7606(2001)113<1580:PTMATC>2.0.CO;2.
- Armijo, R., Meyer, B., King, G.C.P., Rigo, A., and Papanastassiou, D., 1996, Quaternary evolution of the Corinth Rift and its implications for the late Cenozoic evolution of the Aegean: *Geophysical Journal International*, v. 126, p. 11–53, doi: 10.1111/j.1365-246X.1996.tb05264.x.
- Bell, J.W., 1981, Quaternary Fault Map of the Reno 1° by 2° Quadrangle: U.S. Geological Survey Open-File Report 81-982, 62 p.
- Bell, J.W., dePolo, C.M., Ramelli, A.R., Sarna-Wojcicki, A.M., and Meyer, C.E., 1999, Surface faulting and paleoseismic history of the 1932 Cedar Mountain earthquake area, west-central Nevada, and implications for modern tectonics of the Walker Lane: *Geological Society of America Bulletin*, v. 111, p. 791–807, doi: 10.1130/0016-7606(1999)111<0791:SFAPHO>2.3.CO;2.
- Bell, J.W., Caskey, S.J., Ramelli, A.R., and Guerrieri, L., 2004, Pattern and rates of faulting in the central Nevada seismic belt, and paleoseismic evidence for prior beltlike behavior: *Bulletin of the Seismological Society of America*, v. 94, p. 1229–1254, doi: 10.1785/012003226.
- Bennett, R.A., Wernicke, B.P., and Davis, J.L., 1998, Continuous GPS measurements of contemporary deformation across the northern Basin and Range Province: *Geophysical Research Letters*, v. 25, p. 563–566, doi: 10.1029/98GL00128.
- Bennett, R.A., Wernicke, B.P., Niemi, N.A., Friedrich, A.M., and Davis, J.L., 2003, Contemporary strain rates in the northern Basin and Range Province from GPS data: *Tectonics*, v. 22, 1008, doi: 10.1029/2001TC001355.
- Bingler, E.C., 1978, Geologic Map of the Schurz Quadrangle: Nevada Bureau of Mines and Geology Map 60, scale 1:42,000.
- Blewitt, G., Argus, D., Bennett, R., Bock, Y., Calais, E., Craymer, M., Davis, J., Dixon, T., Freymueller, J., Herring, T., Johnson, D., Larson, K., Miller, M., Sella, G., Snay, R., and Tamisiea, M., 2005, A stable North America reference frame (SNARF): First release, UNAVCO-IRIS Joint Workshop: Stevenson, Washington.
- Blewitt, G., Hammond, W.C., and Kreemer, C., 2009, this volume, Geodetic observation of contemporary deformation in the northern Walker Lane: 1. Semipermanent GPS strategy, *in* Oldow, J.S., and Cashman, P.H.,

- eds., Late Cenozoic Structure and Evolution of the Great Basin—Sierra Nevada Transition: Geological Society of America Special Paper 447, doi: 10.1130/2009.2447(01).
- Bourne, S.J., England, P.C., and Parsons, B., 1998, The motion of crustal blocks driven by flow of the lower lithosphere and implications for slip rates of continental strike-slip faults: *Nature*, v. 391, p. 655–659, doi: 10.1038/35556.
- Briggs, R.W., and Wesnousky, S.G., 2004, Late Pleistocene fault slip rate, earthquake recurrence, and recency of slip along the Pyramid Lake fault zone, northern Walker Lane, United States: *Journal of Geophysical Research*, v. 109, p. B08402, doi: 10.1029/2003JB002717.
- Cashman, P.H., and Fontaine, S.A., 2000, Strain partitioning in the northern Walker Lane, western Nevada and northeastern California: *Tectonophysics*, v. 326, p. 111–130, doi: 10.1016/S0040-1951(00)00149-9.
- Caskey, S.J., Bell, J.W., Ramelli, A.R., and Wesnousky, S.G., 2004, Historic surface faulting and paleoseismicity in the area of the 1954 Rainbow Mountain–Stillwater earthquake sequence, central Nevada: *Bulletin of the Seismological Society of America*, v. 94, p. 1255–1275, doi: 10.1785/012003012.
- Clarke, P.J., Davies, R.R., England, P.C., Parsons, B., Billiris, H., Paradissis, D., Veis, G., Cross, P.A., Denys, P.H., Ashkenazi, V., Bingley, R., Kahle, H.-G., Muller, M.-V., and Briole, P., 1998, Crustal strain in central Greece from repeated GPS measurements in the interval 1989–1997: *Geophysical Journal International*, v. 135, p. 195–214, doi: 10.1046/j.1365-246X.1998.00633.x.
- d’Alessio, M.A., Johanson, I.A., Bürgmann, R., Schmidt, D.A., and Murray, M.H., 2005, Slicing up the San Francisco Bay Area: Block kinematics and fault slip rates from GPS-derived surface velocities: *Journal of Geophysical Research*, v. 110, p. B06403, doi: 10.1029/2004JB003496.
- Davies, P., and Blewitt, G., 2000, Methodology for global geodetic time series estimation: A new tool for geodynamics: *Journal of Geophysical Research*, v. 105, p. 11,083–11,100, doi: 10.1029/2000JB900004.
- dePolo, C.M., 1989, Seismotectonics of the White Mountains fault system, east-central California and west-central Nevada [M.Sc. thesis]: Reno, University of Nevada, 354 p.
- dePolo, C.M., and Anderson, J.G., 2000, Estimating the slip rates of normal faults in the Great Basin, USA: *Basin Research*, v. 12, p. 227–240, doi: 10.1046/j.1365-2117.2000.00131.x.
- Dixon, T., Miller, M., Farina, F., Wang, H.Z., and Johnson, D., 2000, Present-day motion of the Sierra Nevada block and some tectonic implications for the Basin and Range Province, North American Cordillera: *Tectonics*, v. 19, p. 1–24, doi: 10.1029/1998TC001088.
- Dixon, T., Norabuena, E., and Hotaling, L., 2003, Paleoseismology and global positioning system: Earthquake-cycle effects and geodetic versus geologic fault slip rates in the Eastern California shear zone: *Geology*, v. 31, p. 55–58, doi: 10.1130/0091-7613(2003)031<0055:PAGPSE>2.0.CO;2.
- Doser, D., 1986, Earthquake processes in the Rainbow Mountain–Fairview Peak–Dixie Valley, Nevada region 1954–1959: *Journal of Geophysical Research*, v. 91, p. 12,572–12,586, doi: 10.1029/JB091iB12p12572.
- Ekren, E.B., and Byers, F.M., Jr., 1984, The Gabbs Valley Range—A well-exposed segment of the Walker Lane in west-central Nevada, in Lintz, J., Jr., ed., *Western Geologic Excursions, Volume 4*: Boulder, Geological Society of America, Fieldtrip Guidebook, p. 204–215.
- Faulds, J.E., Henry, C.D., Coolbaugh, M.F., and Garside, L.J., 2005a, Influence of the late Cenozoic strain field and tectonic setting on geothermal activity and mineralization in the northwestern Great Basin: *Geothermal Resources Council Transactions*, v. 29, p. 353–358.
- Faulds, J.E., Henry, C.D., and Hinz, N.H., 2005b, Kinematics of the northern Walker Lane: An incipient transform fault along the Pacific–North American plate boundary: *Geology*, v. 33, p. 505–508, doi: 10.1130/G21274.1.
- Flesch, L.M., Holt, W.E., Haines, A.J., and Shen-Tu, B., 2000, Dynamics of the Pacific–North American plate boundary in the western United States: *Science*, v. 287, p. 834–836, doi: 10.1126/science.287.5454.834.
- Frey Mueller, J.T., Murray, M.H., Segall, P., and Castillo, D., 1999, Kinematics of the Pacific–North American plate boundary zone, northern California: *Journal of Geophysical Research*, v. 104, p. 7419–7441, doi: 10.1029/1998JB900118.
- Gan, W.J., Svarc, J.L., Savage, J.C., and Prescott, W.H., 2000, Strain accumulation across the Eastern California shear zone at latitude 36°30′N: *Journal of Geophysical Research*, v. 105, p. 16,229–16,236, doi: 10.1029/2000JB900105.
- Garfunkel, Z., 1974, Model for the late Cenozoic tectonic history of the Mojave Desert and its relation to adjacent areas: *Geological Society of America Bulletin*, v. 85, p. 1931–1944, doi: 10.1130/0016-7606(1974)85<1931:MFTLCT>2.0.CO;2.
- Goldsworthy, M., Jackson, J., and Haines, J., 2002, The continuity of active fault systems in Greece: *Geophysical Journal International*, v. 148, p. 596–618, doi: 10.1046/j.1365-246X.2002.01609.x.
- Haines, A.J., and Holt, W.E., 1993, A procedure for obtaining the complete horizontal motions within zones of distributed deformation from the inversion of strain rate data: *Journal of Geophysical Research*, v. 98, p. 12,057–12,082, doi: 10.1029/93JB00892.
- Hammond, W.C., and Thatcher, W., 2004, Contemporary tectonic deformation of the Basin and Range Province, western United States: 10 years of observation with the global positioning system: *Journal of Geophysical Research*, v. 109, p. B08403, doi: 10.1029/2003JB002746.
- Hammond, W.C., and Thatcher, W., 2005, Northwest Basin and Range tectonic deformation observed with the global positioning system, 1999–2003: *Journal of Geophysical Research*, v. 110, p. B10405, doi: 10.1029/2005JB003678.
- Hammond, W.C., and Thatcher, W., 2007, Crustal deformation across the Sierra Nevada, Northern Walker Lane, Basin and Range transition, Western United States, measured with GPS, 2000–2004: *Journal of Geophysical Research*, v. 112, p. B05411, doi: 10.1029/2006JB004625.
- Hammond, W.C., Kreemer, C., and Blewitt, G., 2009, this volume, Geodetic constraints on contemporary deformation in the northern Walker Lane: 3. Central Nevada seismic belt postseismic relaxation, in Oldow, J.S., and Cashman, P.H., eds., *Late Cenozoic Structure and Evolution of the Great Basin—Sierra Nevada Transition*: Geological Society of America Special Paper 447, doi: 10.1130/2009.2447(03).
- Hardyman, R.F., and Oldow, J.S., 1991, Tertiary tectonic framework and Cenozoic history of the central Walker Lane, Nevada, in Raines, G.L., Lisle, R.E., Schafer, R.W., and Wilkinson, W.H., eds., *Geology and Ore Deposits of the Great Basin*, Symposium Proceedings: Reno, Nevada, Geological Society of Nevada, p. 279–301.
- Henry, C.D., Faulds, J.E., and dePolo, C.M., 2007, Geometry and timing of strike-slip and normal faults in the northern Walker Lane, northwestern Nevada and northeastern California: Strain partitioning or sequential extensional and strike-slip deformation?, in Till, A.B., Roeske, S., Sample, J., and Foster, D.A., eds., *Exhumation Associated with Continental Strike-Slip Fault Systems*: Geological Society of America Special Paper 434, p. 59–79, doi: 10.1130/2007.2434(04).
- Hetland, E.A., and Hager, B.H., 2003, Postseismic relaxation across the Central Nevada seismic belt: *Journal of Geophysical Research*, v. 108, 2394, doi: 10.1029/2002JB002257.
- Holt, W.E., Shen-Tu, B., Haines, J., and Jackson, J., 2000, On the determination of self-consistent strain rate fields within zones of distributed deformation, in Richards, M.A., Gordon, R.G., and van der Hilst, R.D., eds., *The History and Dynamics of Global Plate Motions*: American Geophysical Union Geophysical Monograph 121, p. 113–141.
- Holt, W.E., Kreemer, C., Haines, A.J., Estey, L., Meertens, C., Blewitt, G., and Lavallée, D., 2005, Project helps constrain continental dynamics and seismic hazards: *Eos (Transactions, American Geophysical Union)*, v. 86, p. 383–387.
- Ichinose, G.A., Anderson, J.G., Smith, K.D., and Zeng, Y.H., 2003, Source parameters of eastern California and western Nevada earthquakes from regional moment tensor inversion: *Bulletin of the Seismological Society of America*, v. 93, p. 61–84, doi: 10.1785/0120020063.
- Kent, G.M., Babcock, J.M., Driscoll, N.W., Harding, A.J., Dingler, J.A., Seitz, G.G., Gardner, J.V., Mayer, L.A., Goldman, C.R., Heyvaert, A.C., Richards, R.C., Karlin, R., Morgan, C.W., Gayes, P.T., and Owen, L.A., 2005, 60 k.y. record of extension across the western boundary of the Basin and Range Province: Estimate of slip rates from offset shoreline terraces and a catastrophic slide beneath Lake Tahoe: *Geology*, v. 33, p. 365–368, doi: 10.1130/G21230.1.
- Kissel, C., and Laj, C., 1988, The Tertiary geodynamical evolution of the Aegean arc: A paleomagnetic reconstruction: *Tectonophysics*, v. 146, p. 183–201, doi: 10.1016/0040-1951(88)90090-X.
- Kreemer, C., Chamot-Rooke, N., and Le Pichon, X., 2004, Constraints on the evolution and vertical coherency of deformation in the northern Aegean from a comparison of geodetic, geologic and seismologic data: *Earth and Planetary Science Letters*, v. 225, p. 329–346, doi: 10.1016/j.epsl.2004.06.018.
- Kreemer, C., Lavallée, D., Blewitt, G., and Holt, W.E., 2006, On the stability of a geodetic no-net-rotation frame and its implication for the International Terrestrial Reference Frame: *Geophysical Research Letters*, v. 33, doi: 10.1029/2006GL027058.
- Lamb, S.H., 1994, Behavior of the brittle crust in wide plate boundary zones: *Journal of Geophysical Research*, v. 99, p. 4457–4483, doi: 10.1029/93JB02574.
- Langbein, J., Wyatt, F., Johnson, H., Hamann, D., and Zimmer, P., 1995, Improved stability of a deeply anchored geodetic monument for deformation

- monitoring: *Geophysical Research Letters*, v. 22, p. 3533–3536, doi: 10.1029/95GL03325.
- Malservisi, R., Dixon, T.H., La Femina, P.C., and Furlong, K.P., 2003, Holocene slip rate of the Wasatch fault zone, Utah, from geodetic data: *Earthquake cycle effects: Geophysical Research Letters*, v. 30, no. 13, p. 1673, doi: 10.1029/2003GL017408.
- Martinez, L.J., Meertens, C.M., and Smith, R.B., 1998, Rapid deformation rates along the Wasatch fault zone, Utah, from first GPS measurements with implications for earthquake hazard: *Geophysical Research Letters*, v. 25, p. 567–570, doi: 10.1029/98GL00090.
- Mazzotti, S., Dragert, H., Henton, J., Schmidt, M., Hyndman, R., James, T., Lu, Y., and Craymer, M., 2003, Current tectonics of northern Cascadia from a decade of GPS measurements: *Journal of Geophysical Research*, v. 108, p. 2554, doi: 10.1029/2003JB002653.
- McClusky, S.C., Bjornstad, S.C., Hager, B.H., King, R.W., Meade, B.J., Miller, M.M., Monastero, F.C., and Souter, B.J., 2001, Present-day kinematics of the Eastern California shear zone from a geodetically constrained block model: *Geophysical Research Letters*, v. 28, p. 3369–3372, doi: 10.1029/2001GL013091.
- McKenzie, D., and Jackson, J., 1983, The relationship between strain rates, crustal thickening, paleomagnetism, finite strain and fault movements within a deforming zone: *Earth and Planetary Science Letters*, v. 65, p. 182–202, doi: 10.1016/0012-821X(83)90198-X.
- Nicholson, C., Seeber, L., Williams, P., and Sykes, L.R., 1986, Seismic evidence for conjugate slip and block rotation within the San Andreas fault system, southern California: *Tectonics*, v. 5, p. 629–648, doi: 10.1029/TC005i004p00629.
- Niemi, N.A., Wernicke, B.P., Friedrich, A.M., Simons, M., Bennett, R.A., and Davis, J.L., 2004, BARGEN continuous GPS data across the eastern Basin and Range Province, and implications for fault system dynamics: *Geophysical Journal International*, v. 159, p. 842–862, doi: 10.1111/j.1365-246X.2004.02454.x.
- Nur, A., Ron, H., and Scotti, O., 1988, Mechanics of distributed fault and block rotation, in Kissel, C., and Laj, C., eds., *Paleomagnetic Rotations and Continental Deformation*, Volume 254: Series C, *Mathematical and Physical Sciences*: Dordrecht, Kluwer, p. 209–228.
- Oldow, J.S., 1992, Late Cenozoic displacement partitioning in the northwestern Great Basin, in Craig, S.D., ed., *Structure, Tectonics and Mineralization of the Walker Lane*: Reno, Nevada, Geological Society of Nevada, Geological Society of Nevada Symposium Proceedings Volume, p. 17–52.
- Oldow, J.S., 2003, Active transtensional boundary zone between the western Great Basin and Sierra Nevada block, western U.S. Cordillera: *Geology*, v. 31, p. 1033–1036, doi: 10.1130/G19838.1.
- Oldow, J.S., Aiken, C.L.V., Hare, J.L., Ferguson, J.F., and Hardyman, R.F., 2001, Active displacement transfer and differential block motion within the central Walker Lane, western Great Basin: *Geology*, v. 29, p. 19–22, doi: 10.1130/0091-7613(2001)029<0019:ADTADB>2.0.CO;2.
- Pancha, A., Anderson, J.G., and Kreemer, C., 2006, Comparison of seismic and geodetic scalar moment rates across the Basin and Range Province: *Bulletin of the Seismological Society of America*, v. 96, p. 11–32, doi: 10.1785/0120040166.
- Ramelli, A.R., Bell, J.W., dePolo, C.M., and Yount, J.C., 1999, Large-magnitude, late Holocene earthquakes on the Genoa fault, west-central Nevada and eastern California: *Bulletin of the Seismological Society of America*, v. 89, p. 1458–1472.
- Reheis, M.C., and Dixon, T.H., 1996, Kinematics of the Eastern California shear zone: Evidence for slip transfer from Owens and Saline Valley fault zones to Fish Lake Valley fault zone: *Geology*, v. 24, p. 339–342, doi: 10.1130/0091-7613(1996)024<0339:KOTECS>2.3.CO;2.
- Reheis, C., and Sawyer, T.L., 1997, Late Cenozoic history and slip rates of the Fish Lake Valley, Emigrant Peak, and Deep Springs fault zones, Nevada and California: *Geological Society of America Bulletin*, v. 109, p. 280–299, doi: 10.1130/0016-7606(1997)109<0280:LCHASR>2.3.CO;2.
- Savage, J.C., 2000, Viscoelastic-coupling model for the earthquake cycle driven from below: *Journal of Geophysical Research*, v. 105, p. 25,525–25,532, doi: 10.1029/2000JB900276.
- Savage, J.C., Svarc, J.L., and Prescott, W.H., 2004, Interseismic strain and rotation rates in the northeast Mojave domain, eastern California: *Journal of Geophysical Research*, v. 109, p. B02406, doi: 10.1029/2003JB002705.
- Schroeder, J.M., Lee, J., Owen, L.A., and Finkel, R.C., 2003, Pleistocene dextral fault slip along the White Mountains fault zone, California: *Geological Society of America Abstracts with Programs*, v. 35, no. 6, p. 346.
- Schweickert, R.A., Lahren, M.M., Smith, K.D., Howle, J.F., and Ichinose, G., 2004, Transtensional deformation in the Lake Tahoe region, California and Nevada, USA: *Tectonophysics*, v. 392, p. 303–323, doi: 10.1016/j.tecto.2004.04.019.
- Shen, Z.K., Agnew, D.C., and King, R.W., 2003, *The SCEC Crustal Motion Map, Version 3.0*: Los Angeles, California, Southern California Earthquake Center.
- Shen-Tu, B., Holt, W.E., and Haines, A.J., 1998, Contemporary kinematics of the western United States determined from earthquake moment tensors, very long baseline interferometry, and GPS observations: *Journal of Geophysical Research*, v. 103, p. 18,087–18,117, doi: 10.1029/98JB01669.
- Shen-Tu, B., Holt, W.E., and Haines, A.J., 1999, Deformation kinematics in the western United States determined from Quaternary fault slip rates and recent geodetic data: *Journal of Geophysical Research*, v. 104, p. 28,927–28,955, doi: 10.1029/1999JB900293.
- Slemmons, D.B., van Wormer, D., Bell, E.J., and Silberman, M., 1979, Recent crustal movements in the Sierra Nevada–Walker Lane region of California–Nevada: Part I. Rate and style of deformation: *Tectonophysics*, v. 52, p. 561–570, doi: 10.1016/0040-1951(79)90271-3.
- Smith, K.D., von Seggern, D., Blewitt, G., Preston, L., Anderson, J.G., Wernicke, B.P., and Davis, J.L., 2004, Evidence for deep magma injection beneath Lake Tahoe, Nevada–California: *Science*, v. 305, p. 1277–1280, doi: 10.1126/science.1101304.
- Stewart, J.H., 1988, Tectonics of the Walker Lane belt, western Great Basin: Mesozoic and Cenozoic deformation in a zone of shear, in Ernst, W.G., ed., *Metamorphism and Crustal Evolution of the Western United States, Volume 7: Old Tappen*, New Jersey, Prentice-Hall, p. 683–713.
- Stockli, D.F., Dumitru, T.A., McWilliams, M.O., and Farley, K.A., 2003, Cenozoic tectonic evolution of the White Mountains, California and Nevada: *Geological Society of America Bulletin*, v. 115, p. 788–816, doi: 10.1130/0016-7606(2003)115<0788:CTEOTW>2.0.CO;2.
- Surpless, B.E., Stockli, D.F., Dumitru, T.A., and Miller, E.L., 2002, Two-phase westward encroachment of Basin and Range extension into the northern Sierra Nevada: *Tectonics*, v. 21, p. 1002, doi: 10.1029/2000TC001257.
- Svarc, J.L., Savage, J.C., Prescott, W.H., and Murray, M.H., 2002a, Strain accumulation and rotation in western Oregon and southwestern Washington: *Journal of Geophysical Research*, v. 107, p. 2087, doi: 10.1029/2001JB000625.
- Svarc, J.L., Savage, J.C., Prescott, W.H., and Ramelli, A.R., 2002b, Strain accumulation and rotation in western Nevada, 1993–2000: *Journal of Geophysical Research*, v. 107, p. 2090, doi: 10.1029/2001JB000579.
- Thatcher, W., Foulger, G.R., Julian, B.R., Svarc, J., Quilty, E., and Bawden, G.W., 1999, Present-day deformation across the Basin and Range Province, western United States: *Science*, v. 283, p. 1714–1718, doi: 10.1126/science.283.5408.1714.
- Unruh, J., Humphrey, J., and Barron, A., 2003, Transtensional model for the Sierra Nevada fault system, eastern California: *Geology*, v. 31, p. 327–330, doi: 10.1130/0091-7613(2003)031<0327:TMFTSN>2.0.CO;2.
- Wallace, R.E., 1984, Patterns and timing of late Quaternary faulting in the Great Basin Province and relation to some regional tectonic features: *Journal of Geophysical Research*, v. 89, p. 5763–5769, doi: 10.1029/JB089iB07p05763.
- Wallace, R.E., 1987, Grouping and migration of surface faulting and variations in slip rates on faults in the Great Basin province: *Bulletin of the Seismological Society of America*, v. 77, p. 868–876.
- Ward, S.N., 1998, On the consistency of earthquake moment release and space geodetic strain rates: Europe: *Geophysical Journal International*, v. 135, p. 1011–1018, doi: 10.1046/j.1365-246X.1998.t01-2-00658.x.
- Wesnousky, S.G., 2005a, Active faulting in the Walker Lane: *Tectonics*, v. 24, p. TC3009, doi: 10.1029/2004TC001645.
- Wesnousky, S.G., 2005b, The San Andreas and Walker Lane fault systems, western North America: Transpression, transtension, cumulative slip and the structural evolution of a major transform plate boundary: *Journal of Structural Geology*, v. 27, p. 1505–1512, doi: 10.1016/j.jsg.2005.01.015.
- Wesnousky, S.G., Barron, A.D., Briggs, R.W., Caskey, S.J., Kumar, S., and Owen, L., 2005, Paleoseismic transect across the northern Great Basin: *Journal of Geophysical Research*, v. 110, p. B05408, doi: 10.1029/2004JB003283.
- Williams, T.B., Kelsey, H.M., and Freymueller, J.T., 2006, GPS-derived strain in northwestern California: Termination of the San Andreas fault system and convergence of the Sierra Nevada–Great Valley block contribute to southern Cascadia forearc contraction: *Tectonophysics*, v. 413, p. 171–184, doi: 10.1016/j.tecto.2005.10.047.